

# The ghost-gluon vertex in Hamiltonian Yang–Mills theory in Coulomb gauge

Davide R. Campagnari and Hugo Reinhardt  
*Institut für Theoretische Physik, Universität Tübingen,  
Auf der Morgenstelle 14, 72076 Tübingen, Germany*  
(Dated: 23 November 2011)

The Dyson–Schwinger equation for the ghost-gluon vertex of the Hamiltonian approach to Yang–Mills theory in Coulomb gauge is solved at one-loop level using as input the non-perturbative ghost and gluon propagators previously determined within the variational approach. The obtained ghost-gluon vertex is IR finite but IR enhanced compared to the bare one by 15% to 25%, depending on the kinematical momentum regime.

PACS numbers: 11.10.Ef, 12.38.Aw, 12.38.Lg

Keywords: Hamiltonian approach, ghost-gluon vertex, Coulomb gauge

## I. INTRODUCTION

In recent years there have been intensive studies of continuum Yang–Mills theory in the non-perturbative regime. Most of these investigations were carried out either in Landau gauge, using Dyson–Schwinger equations (DSEs) (for reviews see Refs. [1–4]) or functional renormalization group (FRG) flow equations (for reviews see Refs. [5, 6]), or in Coulomb gauge, using DSEs [7]. In addition, variational [8–15] or FRG methods [16] were used in the Hamiltonian formulation of Yang–Mills theory in Coulomb gauge. All those various approaches have in common that the infrared (IR) sector of the theory is dominated by the ghost degrees of freedom, which has been referred to as “ghost dominance”. For this reason the ghost-gluon vertex is of crucial importance in these approaches. Inspired by Taylor’s work [17] showing the non-renormalization of the ghost-gluon vertex in Landau gauge, in all the approaches mentioned above it was tacitly assumed that the ghost-gluon vertex is bare. In Ref. [18] a semi-perturbative calculation of the ghost-gluon vertex was carried out and it was found that its dressing is small even in the IR, a result which is also found on the lattice [19, 20]. Although Taylor’s proof of non-renormalization formally applies also to the ghost-gluon vertex in the Hamiltonian formulation of Yang–Mills theory in Coulomb gauge, the results for the dressing of the ghost-gluon vertex obtained in the functional integral formulation of Yang–Mills theory in Landau gauge [18] cannot be assumed to remain valid also in the Hamiltonian approach in Coulomb gauge. Furthermore, recently it was found within the FRG-approach in Landau gauge that the dressing of the ghost-gluon vertex becomes crucial at high temperatures [21]. Since the high-temperature limit of the 4-dimensional Yang–Mills theory is essentially the 3-dimensional Euclidean Yang–Mills theory and the latter provides an approximation to the Yang–Mills vacuum wave functional in 3 + 1 dimensions<sup>1</sup>[22], the dressing of the ghost-gluon vertex of the Hamiltonian approach in Coulomb gauge should be expected to be also substantial. Therefore, in the present paper we investigate the ghost-gluon vertex of the Hamiltonian approach to Yang–Mills theory in Coulomb gauge. We will solve the DSE for the ghost-gluon vertex using as input the non-perturbative ghost and gluon propagators previously obtained in the variational approach.

In Sec. II we briefly summarize the basic ingredients of the Hamiltonian approach to Yang–Mills theory in Coulomb gauge and also present the results obtained for the ghost and gluon propagators. In Sec. III we give a short derivation of the DSE for the ghost-gluon vertex, and introduce the truncation scheme. Our numerical results are presented in Sec. IV. Some concluding remarks are given in Sec. V.

## II. EQUAL-TIME PROPAGATORS IN COULOMB GAUGE

The Hamiltonian approach to Yang–Mills theory in Coulomb gauge is based on canonical quantization in Weyl gauge  $A_0^a = 0$ , and results in a Schrödinger equation, which has to be solved for the vacuum wave functional  $\psi[A] = \langle A|0\rangle$  of the transverse gauge field  $\partial_i A_i^a = 0$ . Once  $\psi[A]$  is known all static (time-independent) Green’s functions can be evaluated. In Refs. [10, 13] the Yang–Mills Schrödinger equation was solved in an approximate fashion using the variational principle and assuming Gaussian-type trial wave functionals.

---

<sup>1</sup> More precisely, the functional integral of 3-dimensional Euclidean Yang–Mills theory in Landau gauge can be interpreted as the functional integral of the vacuum expectation value of the Hamiltonian approach in Coulomb gauge in 3 + 1 dimensions with a vacuum wave functional given by  $\psi[A] \sim \exp(-\frac{1}{2}S_{\text{YM}}[A])$ , where  $S_{\text{YM}}[A]$  is the classical action of 3-dimensional Euclidean Yang–Mills theory. This wave functional was shown to provide a decent approximation to the true Yang–Mills vacuum wave functional in the mid-momentum regime [23].

In the Hamiltonian formulation of Yang–Mills theory, Coulomb gauge can be implemented in the expectation value of any functional  $K[A]$  of the (spatial components of the) gauge field  $A$  by the Faddeev–Popov method, which results in

$$\langle K[A] \rangle = \int_{\Omega} \mathcal{D}A \mathcal{J}_A |\psi[A]|^2 K[A]. \quad (1)$$

Here,  $\mathcal{J}_A = \text{Det}(G_A^{-1})$  is the Faddeev–Popov determinant with

$$G_A^{-1ab}(\mathbf{x}, \mathbf{y}) = (-\delta^{ab}\partial^2 - g f^{acb} A_i^c(\mathbf{x}) \partial_i) \delta(\mathbf{x} - \mathbf{y}) \quad (2)$$

being the Faddeev–Popov operator. Furthermore,  $g$  is the coupling constant and  $f^{acb}$  are the structure constants of the  $\mathfrak{su}(N_c)$  algebra. The functional integration in Eq. (1) extends over transverse field configurations restricted to the first Gribov region  $\Omega$  or, more precisely, to the fundamental modular region [24]. Moreover, we assume that the wave functional  $\psi[A]$  is properly normalized, such that  $\langle 1 \rangle = 1$ .

To simplify the bookkeeping we will use the compact notation  $A_{i_1}^{a_1}(\mathbf{x}_1) \equiv A(1)$  and assume that a repeated label means summation over colour and spatial indices along with integration over the spatial coordinates,

$$A \cdot B = A(1)B(1) = \int d^3x A_i^a(\mathbf{x}) B_i^a(\mathbf{x}). \quad (3)$$

We use the same convention for indices referring to the ghost field except that the label “1” represents only the colour index  $a_1$  and the spatial coordinate  $\mathbf{x}_1$ .

The gluon propagator  $D$  and the ghost propagator  $G$  are defined by the expectation values

$$D(1, 2) = \langle A(1)A(2) \rangle, \quad G(1, 2) = \langle G_A(1, 2) \rangle. \quad (4)$$

In momentum space we express the gluon propagator by the gluon energy  $\Omega(\mathbf{p})$

$$\langle A_i^a(\mathbf{p}) A_j^b(\mathbf{q}) \rangle =: \delta^{ab} (2\pi)^3 \delta(\mathbf{p} + \mathbf{q}) \frac{t_{ij}(\mathbf{p})}{2\Omega(\mathbf{p})}, \quad (5)$$

where  $t_{ij}(\mathbf{p}) = \delta_{ij} - p_i p_j / \mathbf{p}^2$  is the transverse projector in momentum space. Furthermore the ghost propagator can be represented as

$$G^{ab}(\mathbf{p}) = \delta^{ab} \frac{d(\mathbf{p})}{g\mathbf{p}^2}, \quad (6)$$

where  $d(\mathbf{p})$  is the ghost form factor. Assuming the so-called horizon condition  $d^{-1}(0) = 0$ , the results obtained with Gaussian-type wave functionals [13] show an IR diverging gluon energy  $\Omega(\mathbf{p})$  which can be fitted with Gribov’s formula [25]

$$\Omega(\mathbf{p}^2) = \sqrt{\mathbf{p}^2 + \frac{m_A^4}{\mathbf{p}^2}}, \quad (7)$$

with a mass parameter  $m_A^2 \simeq 0.6 \sigma_c$  (for  $N_c = 2$ ), where  $\sigma_c$  is the Coulomb string tension, i.e. the coefficient of the linear term of the non-Abelian Coulomb potential. These results compare favourably with recent lattice calculations [26]; in particular, the infrared regime of the gluon energy is correctly reproduced.

### III. DERIVATION OF THE GHOST-GLUON VERTEX DSE

In the functional integral formulation of Yang–Mills theory in Landau gauge the DSE for the ghost-gluon vertex has been known for quite some time, see e.g. Ref. [27]. In the Hamiltonian approach in Coulomb gauge the DSE for the ghost-gluon vertex was derived in Ref. [15]. We briefly summarize this derivation in order to fix our notation.

The Faddeev–Popov operator Eq. (2) can be inverted to give the following operator identity for the ghost operator  $G_A$

$$G_A(1, 2) = G_0(1, 2) - G_A(1, 4) A(5) \tilde{\Gamma}_0(5; 4, 6) G_0(6, 2). \quad (8)$$

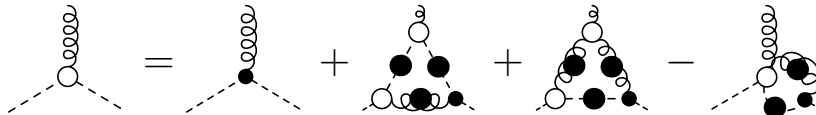


FIG. 1. Diagrammatic representation of the DSE (13). Small filled dots represent connected Green's functions, and small empty dots proper vertex functions.

Here the bare ghost-gluon vertex  $\tilde{\Gamma}_0$  is defined by

$$\tilde{\Gamma}_0(1; 2, 3) = \frac{\delta G_A^{-1}(2, 3)}{\delta A(1)}, \quad (9)$$

and agrees with the lowest order term in the perturbative expansion of the full vertex  $\tilde{\Gamma}$  defined by

$$\langle A(3)G_A(1, 2) \rangle =: -D(3, 3')G(1, 1')G(2', 2)\tilde{\Gamma}(3'; 1', 2'). \quad (10)$$

Taking the v.e.v. of Eq. (8) and using Eq. (10) one obtains the DSE for the ghost propagator  $G$ , which reads

$$G^{-1}(1, 2) = G_0^{-1}(1, 2) - \tilde{\Gamma}(3; 1, 4)D(3, 3')G(4, 4')\tilde{\Gamma}_0(3'; 4', 2). \quad (11)$$

If Eq. (8) is multiplied by a gauge field  $A(3)$  before taking the expectation value, we are led to

$$\langle G_A(1, 2)A(3) \rangle = -\tilde{\Gamma}_0(5; 4, 6)G_0(6, 2)\langle G_A(1, 4)A(5)A(3) \rangle, \quad (12)$$

where we have used  $\langle A \rangle = 0$ . For the left-hand side of Eq. (12) the relation (10) can be used, while the expectation value on the right-hand side can be expanded in terms of vertex functions and propagators [15]. By using the DSE (11) for the ghost propagator, the DSE (12) for the ghost-gluon vertex becomes

$$\begin{aligned} \tilde{\Gamma}(1; 2, 3) &= \tilde{\Gamma}_0(1; 2, 3) + \tilde{\Gamma}(1; 4, 5)G(4', 4)G(5, 5')\tilde{\Gamma}(6'; 5', 3)D(6, 6')\tilde{\Gamma}_0(6; 2, 4') \\ &\quad + \Gamma(1, 4, 5)D(4, 4')D(5, 5')\tilde{\Gamma}(4'; 2, 6)G(6, 6')\tilde{\Gamma}_0(5'; 6', 3) \\ &\quad - \tilde{\Gamma}(1, 5; 2, 4)D(5, 5')G(4, 4')\tilde{\Gamma}_0(5'; 4', 3), \end{aligned} \quad (13)$$

where  $\Gamma(1, 4, 5)$  is the three-gluon vertex, and  $\tilde{\Gamma}(1, 5; 2, 4)$  is the ghost-gluon scattering kernel. Equation (13) is represented diagrammatically in Fig. 1. Note that the vacuum wave functional does not explicitly enter this equation, but only implicitly via the various propagators, in particular the gluon propagator.

Equation (13) must be truncated to be feasible; in a first step we will discard the proper four-point function. Even then, a fully self-consistent solution of the resulting equation together with the DSEs for the propagators is still very expensive and beyond the scope of this work. To get a first estimate of the size of the dressing of the ghost-gluon vertex we will keep the full, non-perturbative propagators but approximate the vertices in the loop terms by their bare form. If the usual assumption of a bare ghost-gluon vertex is justified, the corrections to the bare vertex from the one-loop terms should turn out to be small.

The bare three-gluon vertex is given by the three-gluon kernel  $\gamma_3$  in the exponent of the vacuum wave functional [15]

$$\psi[A] = \exp \left\{ -\frac{1}{2}\omega A^2 - \frac{1}{3!}\gamma_3 A^3 - \dots \right\} \quad (14)$$

which is found from the variational calculation to be given by [15]

$$\gamma_{ijk}^{abc}(\mathbf{p}, \mathbf{q}, \mathbf{k}) = \frac{2f^{abc}T_{ijk}(\mathbf{p}, \mathbf{q}, \mathbf{k})}{\Omega(\mathbf{p}) + \Omega(\mathbf{q}) + \Omega(\mathbf{k})}, \quad (15)$$

where  $T$  is the Lorentz structure of the three-gluon coupling in the Hamiltonian

$$T_{ijk}(\mathbf{p}, \mathbf{q}, \mathbf{k}) = \text{ig}[\delta_{ij}(p - q)_k + \delta_{jk}(q - k)_i + \delta_{ki}(k - p)_j]. \quad (16)$$

Note that  $\gamma_3$  Eq. (15) is the bare part of the three-gluon vertex  $\Gamma_3$  in the sense that it is the leading term in the DSE for  $\Gamma_3$ . However,  $\gamma_3$  Eq. (15) is not the lowest-order perturbative vertex, which is obtained from Eq. (15) when the gluon energy  $\Omega(\mathbf{p})$  is replaced by its perturbative counterpart  $|\mathbf{p}|$ .

After implementing the truncations explained above and extracting the colour structure, Eq. (13) reads in momentum space

$$\begin{aligned} \tilde{\Gamma}_i(\mathbf{k}; \mathbf{p}, \mathbf{q}) = & ig t_{ij}(\mathbf{k}) p_j - t_{ij}(\mathbf{k}) \frac{N_c}{2} \int \tilde{d}\ell (ig p_m) G(\ell) (ig \ell_j) G(\ell + \mathbf{k}) (ig(\ell + k)_n) \frac{t_{mn}(\ell - \mathbf{p})}{2\Omega(\ell - \mathbf{p})} \\ & - t_{ij}(\mathbf{k}) \frac{N_c}{2} \int \tilde{d}\ell (ig p_l) \frac{t_{lm}(\ell)}{2\Omega(\ell)} \frac{2T_{jmn}(\mathbf{k}, \ell, -\ell - \mathbf{k})}{\Omega(\mathbf{k}) + \Omega(\ell) + \Omega(\mathbf{k} + \ell)} \frac{t_{nk}(\ell + \mathbf{k})}{2\Omega(\ell + \mathbf{k})} (ig(p - \ell)_k) G(\ell - \mathbf{p}), \end{aligned} \quad (17)$$

where we have introduced the notation  $\tilde{d}\ell \equiv d^3\ell/(2\pi)^3$ . In Eq. (17)  $\mathbf{k}$ ,  $\mathbf{p}$ , and  $\mathbf{q}$  are respectively the momenta of the gluon and the incoming and outgoing ghost, and momentum conservation  $\mathbf{k} + \mathbf{p} + \mathbf{q} = 0$  is implicitly understood.

We parameterize the full ghost-gluon vertex by a dressing function  $h$  as

$$\tilde{\Gamma}_i(\mathbf{k}; \mathbf{p}, \mathbf{q}) = ig t_{ij}(\mathbf{k}) p_j [1 + h(k^2; p^2, q^2)]. \quad (18)$$

Let us stress that in the present Hamiltonian approach the Coulomb gauge condition is exactly implemented, and the functional integral of the scalar product of the Hilbert space is strictly restricted to (spatially) transverse gauge fields. Therefore, in the present case the ghost-gluon vertex cannot develop a longitudinal part.

Contracting Eqs. (17) and (18) with  $p_i$  and dividing both sides by  $p_i p_j t_{ij}(\mathbf{k})$  we obtain<sup>2</sup>

$$h(k^2; p^2, q^2) = I_1(k^2; p^2, q^2) + g I_2(k^2; p^2, q^2), \quad (19)$$

where

$$I_1 = \frac{N_c}{4p^2[1 - (\hat{\mathbf{k}} \cdot \hat{\mathbf{p}})^2]} \int \tilde{d}\ell p_i t_{ij}(\mathbf{k}) \ell_j \frac{d(\ell)}{\ell^2} \frac{d(\ell + \mathbf{k})}{(\ell + \mathbf{k})^2} \frac{p_m(p + k)_n t_{mn}(\ell - \mathbf{p})}{\Omega(\ell - \mathbf{p})} \quad (20a)$$

is the contribution of the diagram with three ghost-gluon vertices, and

$$I_2 = \frac{N_c}{4p^2[1 - (\hat{\mathbf{k}} \cdot \hat{\mathbf{p}})^2]} \int \tilde{d}\ell \frac{p_i p_j (p + k)_k t_{il}(\mathbf{k}) t_{jm}(\ell) t_{kn}(\ell + \mathbf{k}) T_{lmn}(\mathbf{k}, \ell, -\ell - \mathbf{k})}{\Omega(\ell)\Omega(\ell + \mathbf{k})[\Omega(\mathbf{k}) + \Omega(\ell) + \Omega(\ell + \mathbf{k})]} \frac{d(\ell - \mathbf{p})}{(\ell - \mathbf{p})^2} \quad (20b)$$

is the contribution of the diagram containing the three-gluon vertex; the latter is multiplied by the coupling constant  $g$  due to the parameterization of the ghost propagator, see Eq. (6). It should be remarked here that the integrals Eqs. (20) are UV finite and need not to be renormalized. In the subsequent numerical calculations we will consider two classes of kinematic configurations, namely

$$h(p^2; p^2, xp^2) \quad \text{and} \quad h(xp^2; p^2, p^2), \quad (21)$$

where  $x$  is restricted to the interval  $x \in [0, 4]$  due to momentum conservation.

Before concluding this section we investigate the IR limit of the ghost-gluon vertex. In the IR the ghost and gluon propagator can be parameterized as

$$d(\mathbf{p} \rightarrow 0) \sim \frac{m_c^\beta}{|\mathbf{p}|^\beta}, \quad \Omega(\mathbf{p} \rightarrow 0) \sim \frac{m_A^{1+\alpha}}{|\mathbf{p}|^\alpha}, \quad (22)$$

with  $\beta > 0$  to fulfil the horizon condition  $d^{-1}(0) = 0$ . These IR exponents obey the sum rule  $1 + \alpha = 2\beta$  [12, 28, 29]. Inserting the IR ansatzes Eq. (22) into Eqs. (20) we find that in the limit of vanishing momenta the form factor of the ghost gluon vertex approaches the finite expression

$$h(0; 0, 0) = \frac{N_c}{24(1 + \beta)\pi^2} \left( \frac{m_c}{m_A} \right)^{2\beta}. \quad (23)$$

A fit to the numerical data [13] for the propagators with  $N_c = 2$  and the solution  $\beta = 1$  yields  $m_c \simeq 4.97\sqrt{\sigma_c}$  while  $m_A$  was given below Eq. (7). Plugging these values into Eq. (23) yields an IR value of 0.174 for the ghost-gluon-vertex form factor  $h$ . The numerical data shown in the next section confirm this value.

---

<sup>2</sup> The limit  $\hat{\mathbf{p}} \cdot \hat{\mathbf{k}} \rightarrow \pm 1$  is finite.

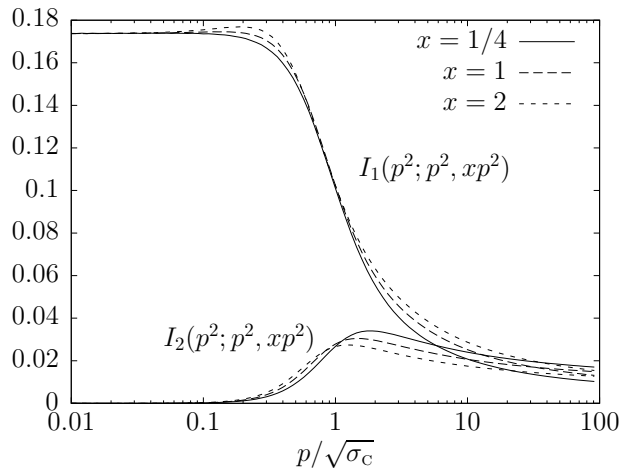


FIG. 2. Numerical results for the two integrals contributing to the form factor of the ghost-gluon vertex  $h(p^2; p^2, xp^2)$ , see Eqs. (19) and (20).

#### IV. NUMERICAL RESULTS

For the ghost and gluon propagators we use the results obtained previously in the variational approach [13] as input. In particular, for the gluon propagator we use the Gribov formula [Eq. (7)], while for the ghost form factor [Eq. (6)] we use the parameterization [15, 30]

$$d(\mathbf{p}) = a \sqrt{\frac{1}{\mathbf{p}^2/\sigma_c} + \frac{1}{\ln(\mathbf{p}^2/\sigma_c + c)}}, \quad (24)$$

with  $a = 4.97$  and  $c = 16$ . The factor  $g$  has been absorbed in the ghost propagator as explained in Refs. [10, 13]. This has the advantage that the coupling constant  $g$  disappears from the coupled system of equations, as long as gluonic vertices are ignored. However, since the diagram containing the three-gluon vertex has a prefactor  $g^2$  but only a single ghost propagator in the integral, in Eq. (19) there remains an explicit factor  $g$ . We will take the coupling at the renormalization point  $\mu = 2.4\sqrt{\sigma_c}$  [13]  $g_r = 3.5$ .

Figure 2 shows the values of the two integrals  $I_1$  and  $I_2$  separately, for equal ghost and gluon momentum. The integral  $I_1$  involving three ghost-gluon vertices approaches the IR value evaluated in Eq. (23), showing a modest dependence on the kinematic configuration. At high momenta it drops off logarithmically, due to the anomalous dimension of the ghost propagator. The integral  $I_2$  involving the three-gluon vertex vanishes in the deep IR, due to the IR divergence of the gluon energy  $\Omega(\mathbf{k})$  in the denominator, see Eqs. (17) and (20), and drops off in the UV more slowly than the ghost-loop term ( $1/\sqrt{\ln p}$  instead of  $1/\ln p$ ), since it contains only one ghost propagator. Figure (3) shows the total form factor  $h(p^2; p^2, xp^2)$ .

More interesting is the kinematic configuration where the ghost legs have momenta of equal magnitude and the gluon momentum is varied, see Fig. 4. One observes that the maximum in the mid-momentum regime gets stronger as the gluon momentum approaches zero. If the gluon momentum is very small but not zero (dashed line with  $x = 10^{-4}$  in Fig. 4), the form factor is almost indistinguishable from the case of vanishing gluon momentum in the IR and in the mid-momentum regime; however, at higher momenta the term involving the three-gluon vertex dominates, and we observe again the  $(\ln p)^{-1/2}$  behaviour.

As explained in the footnote of the introduction, the 3-dimensional Euclidean Yang–Mills theory in Landau gauge is equivalent to the Hamiltonian approach in Coulomb gauge in 3+1 dimensions using a specific vacuum wave functional, which is a decent approximation to the true one in the mid-momentum regime. Therefore we can compare our results with lattice data from 3-dimensional Landau gauge [20], see Fig. 5. The vertex there displays a maximum in the mid-momentum regime which is somewhat stronger than in our work; furthermore, the form factor from the lattice seems to approach zero or even a small negative value in the IR. Qualitatively similar results have been obtained in 3- and 4-dimensional Landau gauge both in the continuum [18] and on the lattice [19].

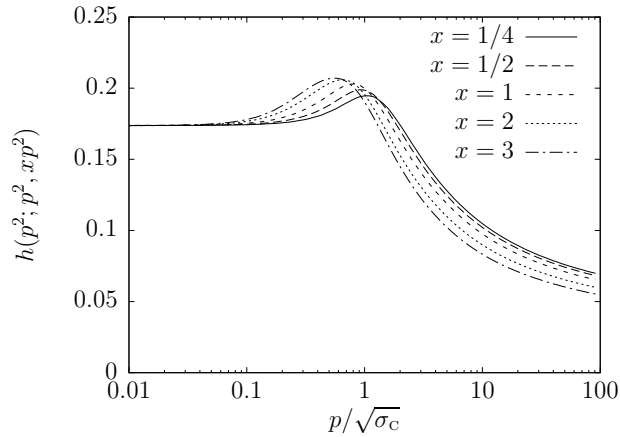


FIG. 3. Numerical results for the form factor  $h(p^2; p^2, xp^2)$  of the ghost-gluon vertex with equal ghost and gluon momentum.

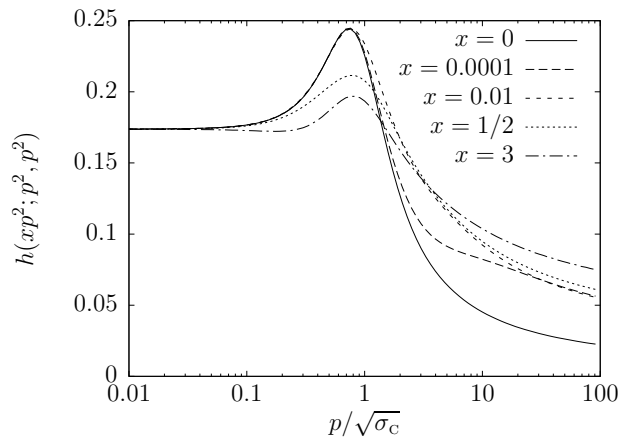


FIG. 4. Numerical results for the form factor  $h(xp^2; p^2, p^2)$  with equal incoming and outgoing ghost. Explanation see text.

## V. CONCLUSIONS

We have investigated the ghost-gluon vertex of the Hamiltonian approach to Yang–Mills theory in Coulomb gauge. The DSE for the ghost-gluon vertex was solved in one-loop truncation using the non-perturbative ghost and gluon propagators obtained previously in the variational approach assuming a bare ghost-gluon vertex. The dressing of the ghost-gluon vertex was found to increase the vertex between 15% and 25% in the IR and to vanish asymptotically in the UV. Since the gluon propagator obtained in the variational approach with a bare ghost-gluon vertex is qualitatively similar to that obtained on the lattice [26] (which contains the full dressing of vertices) we expect that a fully self-consistent solution of the coupled DSEs for the propagators and vertices yield similar results for the ghost-gluon vertex as obtained in the present paper. Finally it will be interesting to extend the present studies to finite temperatures [31] to see whether there is a similar change of the dressing of the ghost-gluon vertex at high temperatures as observed in the FRG approach in Landau gauge [21].

## ACKNOWLEDGMENTS

The authors are grateful to P. Watson and M. Quandt for useful discussions and for a critical reading of the manuscript. They also thank A. Maas for providing the lattice data from Ref. [20]. This work has been supported by

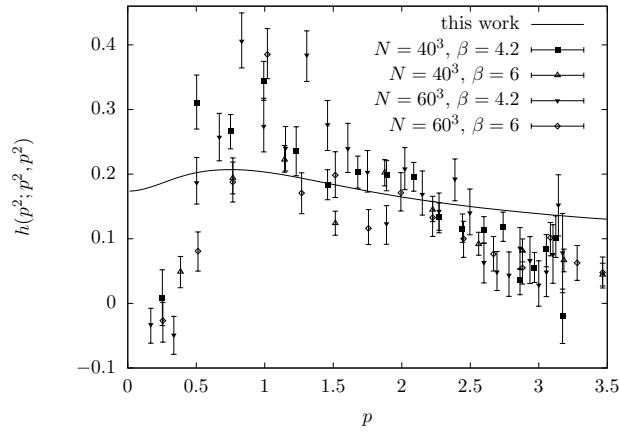


FIG. 5. Comparison of our result for the form factor of the ghost-gluon vertex to lattice data from Ref. [20] at the symmetric point,  $h(p^2; p^2, p^2)$ .

the Deutsche Forschungsgemeinschaft under contract no. DFG-Re856/6-3.

- 
- [1] R. Alkofer and L. von Smekal, Phys. Rept. **353**, 281 (2001).  
[2] C. S. Fischer, J. Phys. **G32**, R253 (2006).  
[3] L. von Smekal, arXiv:0812.0654[hep-th] (2008).  
[4] D. Binosi and J. Papavassiliou, Phys. Rept. **479**, 1 (2009).  
[5] J. M. Pawłowski, Annals Phys. **322**, 2831 (2007).  
[6] H. Gies, arXiv:hep-ph/0611146 (2006).  
[7] P. Watson and H. Reinhardt, Phys. Rev. **D75**, 045021 (2007); Phys. Rev. **D76**, 125016 (2007); Phys. Rev. **D77**, 025030 (2008).  
[8] D. Schütte, Phys. Rev. **D31**, 810 (1985).  
[9] A. P. Szczepaniak and E. S. Swanson, Phys. Rev. **D65**, 025012 (2001).  
[10] C. Feuchter and H. Reinhardt, Phys. Rev. **D70**, 105021 (2004); arXiv:hep-th/0402106.  
[11] H. Reinhardt and C. Feuchter, Phys. Rev. **D71**, 105002 (2005).  
[12] W. Schleifenbaum, M. Leder, and H. Reinhardt, Phys. Rev. **D73**, 125019 (2006).  
[13] D. Epple, H. Reinhardt, and W. Schleifenbaum, Phys. Rev. **D75**, 045011 (2007).  
[14] H. Reinhardt, Phys. Rev. Lett. **101**, 061602 (2008).  
[15] D. R. Campagnari and H. Reinhardt, Phys. Rev. **D82**, 105021 (2010).  
[16] M. Leder, J. M. Pawłowski, H. Reinhardt, and A. Weber, Phys. Rev. **D83**, 025010 (2011).  
[17] J. C. Taylor, Nucl. Phys. **B33**, 436 (1971).  
[18] W. Schleifenbaum, A. Maas, J. Wambach, and R. Alkofer, Phys. Rev. **D72**, 014017 (2005).  
[19] A. Cucchieri, T. Mendes, and A. Mihara, JHEP **12**, 012 (2004).  
[20] A. Cucchieri, A. Maas, and T. Mendes, Phys. Rev. **D77**, 094510 (2008).  
[21] L. Fister and J. M. Pawłowski, to be published.  
[22] J. P. Greensite, Nucl. Phys. **B158**, 469 (1979).  
[23] M. Quandt, H. Reinhardt, and G. Burgio, Phys. Rev. **D81**, 065016 (2010).  
[24] D. Zwanziger, Nucl. Phys. **B412**, 657 (1994).  
[25] V. N. Gribov, Nucl. Phys. **B139**, 1 (1978).  
[26] G. Burgio, M. Quandt, and H. Reinhardt, Phys. Rev. Lett. **102**, 032002 (2009).  
[27] J. Smit, Phys. Rev. **D10**, 2473 (1974).  
[28] D. Zwanziger, Phys. Rev. **D65**, 094039 (2002).  
[29] C. Lerche and L. von Smekal, Phys. Rev. **D65**, 125006 (2002).  
[30] P. Watson and H. Reinhardt, Phys. Rev. **D82**, 125010 (2010).  
[31] H. Reinhardt, D. Campagnari, and A. Szczepaniak, Phys. Rev. **D84**, 045006 (2011). J. Heffner, H. Reinhardt, and D. R. Campagnari, to be published.